Contents lists available at GrowingScience

Current Chemistry Letters

homepage: www.GrowingScience.com

Synthesis, characterization, and biological activities of five new trivalent lanthanide complexes of hydrazine and 3,3'-thiodipropanoic acid

K. Kumar[a*], S. Murugesan[a], T. Muneeswaran[b], C. M. Ramakritinan[b]

[a]*Department of Inorganic Chemistry, School of Chemistry, Madurai Kamaraj University Madurai, 625 021, India*
[b]*Department of Marine and Coastal Studies, School of Energy, Environment and Natural Resources, Madurai Kamaraj University, Pudumadam, India*

C H R O N I C L E

Article history:
Received December 25, 2022
Received in revised form
January 28, 2023
Accepted May 12, 2023
Available online
May 12, 2023

Keywords:
Hydrazine
Carboxylic Acid
Lanthanoids
Metal Complexes
Biological Activity

A B S T R A C T

Some new hydrazine complexes of trivalent lanthanide 3,3'-thiodipropanoates of empirical formulae $[M(N_2H_5)(tdp)_2]$ and $[Pr(N_2H_5)(tdp)_2{\cdot}H_2O]$, where M = La, Ce, Sm and Nd, H_2tdp = 3,3'-thiodipropanoic acid, have been prepared and characterized by elemental analysis, mass, FTIR, Raman and electronic spectral, powder X-ray diffraction, scanning electron microscopy (SEM) and simultaneous TG–DTA techniques. The presence of bidentate carboxylate anion and coordinated N_2H_5 in these complexes are confirmed by IR spectra. TGA/DTA results confirmed that all the rare earth metal complexes give the corresponding metal carbonate (heating up to 1000 °C) through a metal oxalate intermediate. SEM images of Pr_2O_3 residue obtained from its complex show nano-sized clusters, thus the complex may be used as a precursor for nano-Pr_2O_3 preparation. The synthesized complexes show good antimicrobial activity against six bacteria (*Bacillus cereus, Staphylococcus aureus, Proteus vulgaris, Pseudomonas aeruginosa, Escherichia coli,* and *Serratia species*) and four fungi (*Candida albicans, Aspergillus niger*, *Aspergillus fumigatus,* and *Penicillium variance*) as assessed by *in vitro* biological activity.

1. Introduction

Our interest in bioinorganic and coordination chemistry often stems from the complications present in the inner transition metals.[1,2] For instance, the observation of various kinds of biological activities exerted by lanthanide metal complexes attracted newer minds around the world to explore deeper and deeper.[3-5] Some rare earth metal complexes are used in the biomedical analysis as contrast agents in Magnetic Resonance Imaging (MRI) and effective catalysts in the hydrolytic cleavage of phosphate ester bonds.[6,7] The rare earth metal ions exhibit several interesting optical, electrical, and magnetic inherency properties owing to their superior electronic structure. The wide potential applications of lanthanides with appropriate organic ligands were mainly associated with the utilization of their luminescence property.[8-11] Prior studies inferred that the better electronic configuration of rare earth metal complexes resulted in the observation of very good physical and chemical properties, which, in turn, aided the deliverance of anti-inflammation, antitumor and anti-thrombogenic potency.[12-14]

Intriguingly, the properties of rare earth metal ions can be modified (altered and enhanced) by tuning the interactions between lanthanide ions and carboxylic acid ligands.[15] In addition to functioning as a chelating ligand, 3,3'-thiodipropanoic acid (Commonly called thiodipropanoic acid) can function as a bridging ligand for the assembly of coordination complexes. The transition metal complexes of Cr(III), Co(II), Ni(II), and Cu(II) with 3,3'-thiodipropanoic acid have been reported in the literature.[16] Coordination complexes of Zn(II) with 3,3'-thiodipropanoic acid and bipyridyl ligand were synthesized,

* Corresponding author.
E-mail address kumar05mrk@gmail.com (K. Kumar)

doi: 10.5267/j.ccl.2023.5.003

structurally characterized and their luminescence properties were evaluated.[17] Numerous types of the binding capability of 3,3'-thiodipropanoic acid with transition metals including spectral studies were demonstrated.[18] The luminescent properties of rare earth metal complexes of thiodipropanoic acid with aminoguanidine are studied.[19] The different possible coordination manners of 3,3'-thiodipropanoic acid (H_2tdp), acting as chelating (a–c) and bridging (d–g) ligands with metal ions are shown in **Fig. 1**.

Surface properties and catalytic activity of various metal oxides such as, Cobalt, Palladium, Chromium, Cerium, and Zirconium and several mixed oxides were reported.[20,21] Various metal oxides were synthesized by different methods like, the wetness impregnation method, Classical ion exchange method, ultrasound modification ion exchange method, and sonochemical sol-gel method were also reported.[22,23] These metal oxide and mixed metal oxides were utilized as a catalyst in several applications such as, methane combustion, n-nonane combustion activity, etc.[24] The presence of hydrazine as a neutral monodentate, bidentate bridged, and monodentate $N_2H_5^+$ cation ligand in various complexes.[25-27] The thermal decomposition of metal carboxylates with hydrazine ligands is of increasing importance because they serve as precursors to fine-particle metal oxides and metal carbonates.[28,29] Studies using hydrazine as a co-ligand for carboxylate complexes of transition and lanthanide metals are growing. For instance, complexes of formic acid,[30] acetic acid,[31] propionic acid,[32] glycolic acid,[33] salicylic acid,[34] tri- and tetra- carboxylic acid,[35,36] naphthoxy and hydroxyl napthoic acid[37,38] with hydrazine as co-ligand are reported. Upto our knowledge, there are no reports available, until now, on the rare earth metal complexes of thiodipropanoic acid with hydrazine as a co-ligand.

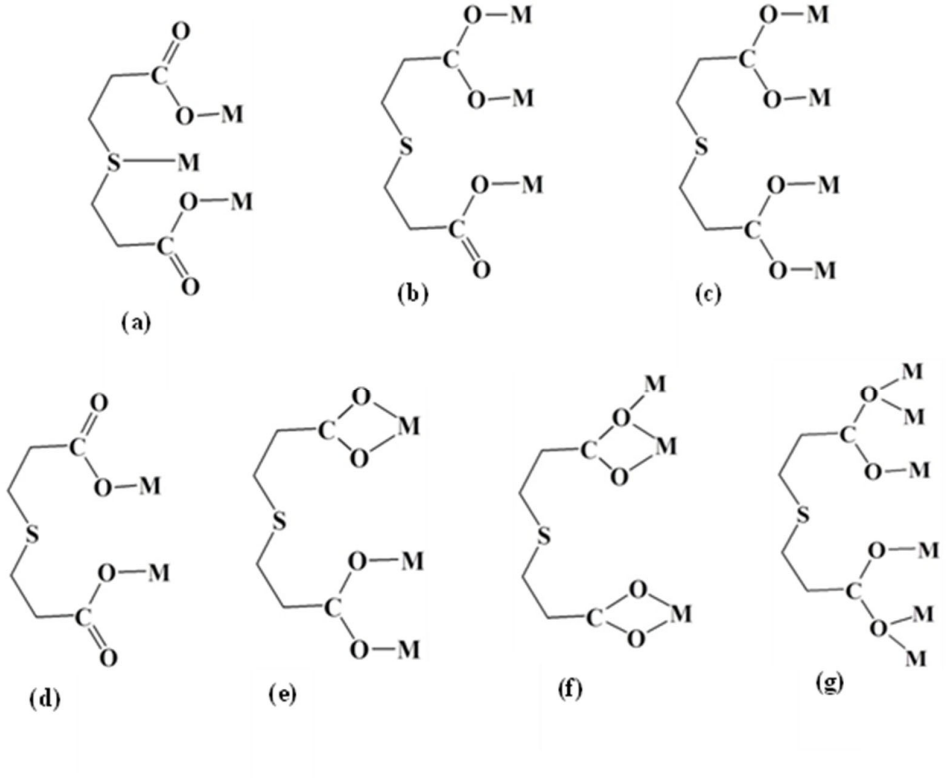

Fig. 1. Typical coordination modes of 3,3'-thiodipropanoic acid (H_2tdp).[17, 39-42]

The present study is focused on the maiden synthesis, characterization, and antimicrobial activity of rare earth metal complexes of hydrazine and sulphur containing heteroaliphatic dicarboxylic acid, namely, thiodipropanoic acid (H_2tdp), [$S(CH_2CH_2COOH)_2$].

2. Results and Discussion

The trivalent complexes of La, Ce, Sm, Pr, and Nd were prepared by the reaction between the aqueous solution of the corresponding metal nitrate hexahydrate and an aqueous solution of mixed ligands of hydrazine hydrate and 3,3'-thiodipropanoic acid.

$M(NO_3)_3{\cdot}6H_2O + 2S(CH_2CH_2COOH)_2 + N_2H_4{\cdot}H_2O \rightarrow [M(N_2H_5)(S(CH_2CH_2COO)_2)_2] + 3HNO_3 + 7H_2O \rightarrow (1)$

where M = La, Ce, Sm and Nd

$Pr(NO_3)_3.6H_2O + 2S(CH_2CH_2COOH)_2 + N_2H_4.H_2O \rightarrow [Pr(N_2H_5)(S(CH_2CH_2COO)_2)_2{\cdot}H_2O] + 3HNO_3 + 6H_2O \rightarrow (2)$

All the complexes were obtained as polycrystalline-amorphous composite powders having stability in atmospheric air and were found to be insensitive to light exposure. Further, these complexes were insoluble in aqueous and organic solvents such as ethanol, acetone, and chloroform. All the prepared complexes were frugally soluble in the methanol-acetylacetone solvent system. Based on the elemental (CHNS) analysis, hydrazine, and metal contents, the compositions of these complexes were formulated **(Table 1)**. For confirmation of the proposed molecular formula of the complexes, mass spectral analyses were carried out. The mass spectra of the Ce(III), La(III) and Sm(III) complexes **(Figs. S1–S3)** displayed molecular ion peaks at m/z 558.85 $(m+CH_3OH+H)^+$, 588.42 $(m+ACN+Na)^+$ and 582.84 $(m+2Na+H)^+$ respectively, which match with the molecular formulae of $CeC_{12}H_{21}O_8N_2S_2$, $LaC_{12}H_{21}O_8N_2S_2$ and $SmC_{12}H_{21}O_8N_2S_2$ respectively.

Table 1. Analytical data of the prepared complex

Compound (Colour)	Molecular weight g/mol	Proposed molecular formula	Found (calculated)% C (CHNS)	H (CHNS)	N (CHNS)	S (CHNS)	M (ICP-OES)	Hydrazine
$La(N_2H_5)(tdp)_2$ (Colourless)	524.36	$LaC_{12}H_{21}O_8N_2S_2$	26.9(27.4)	3.8(4.0)	4.7(5.3)	12.0(12.2)	25.9(26.4)	6.2(6.1)
$Ce(N_2H_5)(tdp)_2$ (Dirty white)	525.56	$CeC_{12}H_{21}O_8N_2S_2$	26.8(27.3)	3.5(3.9)	4.8(5.3)	11.8(12.1)	26.2(26.6)	6.2(6.1)
$Sm(N_2H_5)(tdp)_2$ (Colourless)	535.86	$SmC_{12}H_{21}O_8N_2S_2$	26.4(26.8)	3.5(3.9)	4.8(5.2)	11.6(11.9)	27.8(28.0)	6.1(5.9)
$Pr(N_2H_5)(tdp)_2{\cdot}H_2O$ (Light green)	544.36	$PrC_{12}H_{23}O_9N_2S_2$	26.0(26.4)	4.1(4.2)	4.7(5.1)	11.5(11.7)	25.7(25.8)	6.1(5.8)
$Nd(N_2H_5)(tdp)_2$ (Light blue)	529.66	$NdC_{12}H_{21}O_8N_2S_2$	26.7(27.1)	3.6(3.9)	4.8(5.2)	11.6(12.0)	27.0(27.2)	6.2(6.0)

2.1. Infrared spectral analysis

Typical IR spectra observed for 3,3'-thiodipropanoic acid, $La(N_2H_5)(tdp)_2$, $Ce(N_2H_5)(tdp)_2$, $Sm(N_2H_5)(tdp)_2$, $Pr(N_2H_5)(tdp)_2.H_2O$ and $Nd(N_2H_5)(tdp)_2$ are provided in **Fig. 2**, and the important IR absorption frequencies observed for the ligand and its metal complexes prepared are given in **Table S1**. It was observed that all the prepared complexes displayed a band in the range of 3409–3428 cm^{-1} which is assigned to N—H stretching frequencies of hydrazine moieties. The stretchings of carboxylate (ν_{asym} and ν_{sym}) are observed in the region 1533–1552 and 1422–1432 cm^{-1} respectively, in all the complexes, with $\Delta\nu$ between them of 111–120 cm^{-1}, displayed the bidentate coordination of both carboxylate groups in the dianion.[43] The N—N stretching frequency of hydrazinium moiety is seen at 932–940 cm^{-1} indicating its mono-dentate nature.[44] The entire complexes display strong bands in the zone of 470–526 cm^{-1} due to M—O stretching vibration of the complexes. The aliphatic C—S stretching band observed at around 665 cm^{-1} in the ligand does not display any shift signifying the presence of uncoordinated sulphur atom in these complexes. This may be due to the steric hindrance caused by the presence of large bulky carboxylic groups on each end of the molecule.[45]

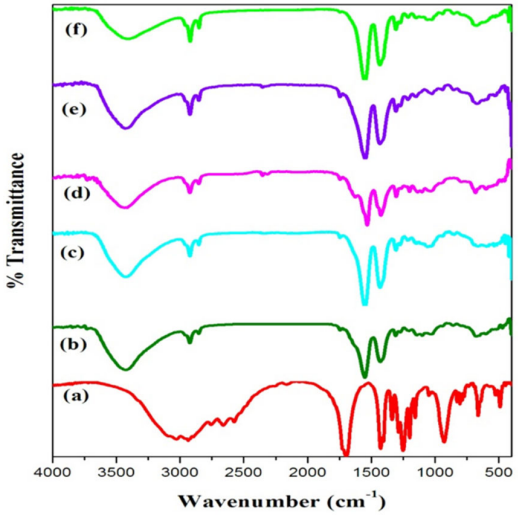

Fig. 2. IR Spectra of (a) 3,3'-thiodipropanoic acid, (b) $La(N_2H_5)(tdp)_2$, (c) $Ce(N_2H_5)(tdp)_2$, (d) $Sm(N_2H_5)(tdp)_2$, (e) $Pr(N_2H_5)(tdp)_2{\cdot}H_2O$ and (f) $Nd(N_2H_5)(tdp)_2$.

2.2. Raman spectra

The obtained Raman spectra of 3,3'-thiodipropanoic acid and lanthanide 3,3'-thiodipropanoate are shown in **Fig. 3** and the observed IR and Raman spectral data and their assignments are provided in **Table S2**. The observed Raman spectrum of 3,3'-thiodipropanoic acid displays the characteristic band of the stretching vibration of the carboxylic hydroxyl group ($\nu(OH)_{COOH}$ 2967 cm^{-1}), the carbonyl group ($\nu(C=O)$ 1690 cm^{-1}) and out-of-plane bending vibrations of the carboxylic acid group ($\gamma(OH)_{COOH}$ 914 cm^{-1}). The Raman spectra of metal complexes do not display the characteristic bands of COOH bending or stretching, instead bands due to the COO^- group appear which evidenced that the carboxylate groups are involved in the chelation with the lanthanide metal ion. Replacement of hydrogen in the carboxylic group with a metal ion causes a variation in the bond strengths of carboxylate groups and hence the complexes show carboxylate stretching vibration at lower frequencies than that observed for the free ligand.

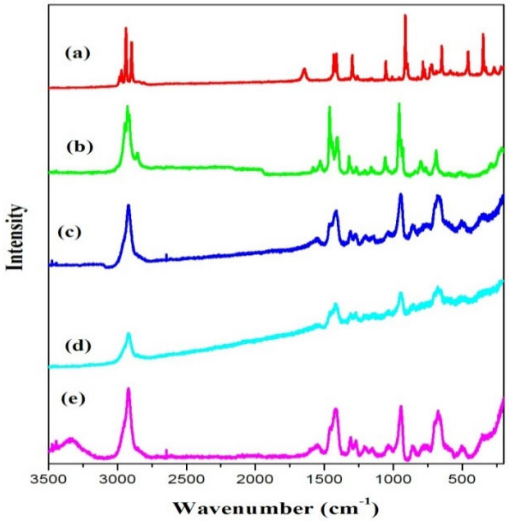

Fig. 3. Raman spectra of 3,3'-thiodipropanoic acid (a), and the complexes of Praseodymium (b), Samarium (c), Lanthanum (d), and Neodymium (e).

The presence of a band in the region of 1431–1463 cm^{-1} for acid and its complexes is due to $\delta(CH_2)$ in-plane-bending vibration. Further, the observation of bands in the region of 1200–1274 cm^{-1} is the bands derived from stretching vibrations of the aliphatic chain ($\nu(C–C)$). These bands are observed at about similar wavenumbers in the spectra of both acid and complexes. The carboxylic acid and its complexes exhibit a strong band in the range of ~660 cm^{-1} corresponding to the stretching vibration of the aliphatic carbon-sulfur chain ($\nu(C–S)$).

2.3. Electronic Spectra

The metal complexes were insoluble in water and organic solvents, and hence their electronic spectra were recorded in the solid phase and the observed electronic spectra of Pr^{III}, $Nd^{III,}$ and Sm^{III} complexes are shown in **Fig. 4**.

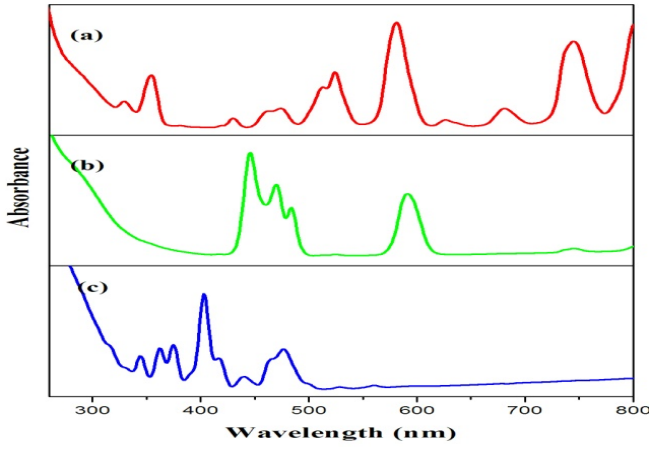

Fig. 4. Electronic spectra of (a) $[Nd(tdp)_2(N_2H_5)]$; (b) $[Pr(tdp)_2(N_2H_5)\cdot H_2O]$; (c) $[Sm(tdp)_2(N_2H_5)]$.

The Sm(III) complex exhibit bands at 28985, 27624, 26737, 24813, 24038, 22779, and 21008 cm^{-1} corresponding to three spin allowed and four spin forbidden transitions while the Pr(III) complex show four bands at 22421, 21276, 20661 and 16920 cm^{-1} attributable to three spin allowed and one spin forbidden transitions. The Nd(III) complex displays eight bands at 23310, 21052, 19531, 19083, 17211, 15974, 14705, and 13333 cm^{-1}. The electronic spectral data of the complexes and their assignments were consolidated in **Table S3**. The La(III) and Ce(III) complexes do not display any characteristic absorption in the visible region. On comparing the absorption spectra of Sm, Pr, and Nd complexes with the data for the corresponding aqua-ions, the Pr^{III}, Nd^{III}, and Sm^{III} complexes show a significant red shift in the λ_{max} values from those of the corresponding aqua ions.[46] This is presumably due to the Nephelauxetic effect[47] which is regarded as a measure of covalency of the bonding between the metal ions and the ligands and thus indicates the formation of the complex.

2.4. Thermal analysis

The simultaneous TG-DTA of the La^{3+}, Ce^{3+}, Sm^{3+}, Pr^{3+}, and Nd^{3+} complexes were carried out to study their thermal stability and decomposition behavior, and the representative thermograms of La(III) and Pr(III) are shown in **Fig. 5**. The complexes of La(III), Ce(III), Sm(III), and Nd(III) displayed similar patterns of thermal decomposition. These thermal curves exhibit mass losses in three steps and the thermal events corresponding to these losses are due to chemical phenomena. The first step, which arises in the temperature range of 50–240 °C ascribed to the loss of hydrazinium moiety to give the corresponding metal carboxylate as an intermediate. In DTA this was detected as an endotherm around 150 °C. The second decomposition step corresponds to the elimination of organic moieties in the range of 240–750 °C which resulted in the formation of the corresponding metal oxalate as an intermediate. In DTA, this loss of organic moiety is seen as an exotherm around 400 °C. This intermediate further decomposes to give the corresponding metal carbonate in the range of 760–970 °C. The thermal analytical data and derived decomposition products are summarized in **Table S4**.

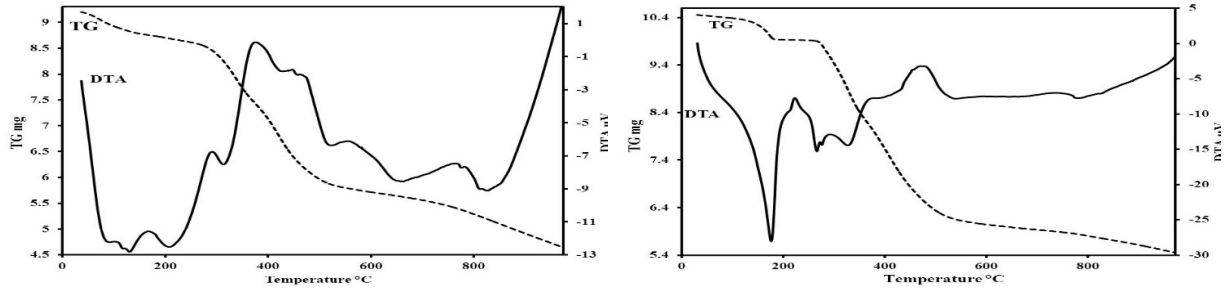

Fig. 5. Simultaneous TG–DTA curves of (a) $La(N_2H_5)(tdp)_2$ and (b) $Pr(N_2H_5)(tdp)_2 \cdot H_2O$.

The degradation of $Pr(N_2H_5)(tdp)_2 \cdot H_2O$ complex also consisted of three steps, but with different decomposition products. Initially, loss of water molecules occurs in the range of 100–200 °C to give the corresponding metal hydrazinium carboxylate as an intermediate. In DTA, it was observed as an endotherm around 170 °C. The occurrence of dehydration at slightly high temperatures confirmed the presence of one coordinated water molecule in the complex. The second level of degradation occurred in the 270–760 °C range that corresponds to the simultaneous dehydrazination and removal of organic matter to produce respective metal oxalate as an intermediate. This intermediate further decomposes to give the praseodymium carbonate in the 760–970 °C temperature range. The scheme of decomposition in the N_2 atmosphere, as derived from thermal studies is given below.

$$[Ln(N_2H_5)(tdp)_2] \xrightarrow[\text{Dehydrazination}]{\text{50-240 °C}} [Ln(tdp)_2]$$

$$[Ln(tdp)_2] \xrightarrow[\text{Organics decomposition}]{\text{240-750 °C}} 1/2Ln_2(C_2O_4)_3$$

$$Ln_2(C_2O_4)_3 \xrightarrow[\text{-3CO}]{\text{760-970 °C}} Ln_2(CO_3)_3$$

where Ln = La, Ce, Nd and Sm

$$[Pr(N_2H_5)(tdp)_2.H_2O] \xrightarrow[\text{Dehydration}]{\text{100-200 °C}} [Pr(N_2H_5)(tdp)_2]$$

$$[Pr(N_2H_5)(tdp)_2] \xrightarrow[\text{Organics decomposition}]{\text{270-760 °C}} 1/2Pr_2(C_2O_4)_3$$

$$Pr_2(C_2O_4)_3 \xrightarrow[\text{-3CO}]{\text{760-970 °C}} Pr_2(CO_3)_3$$

2.5. Powder X-ray diffraction studies

Powder XRD patterns of the La(III), Ce(III), Pr(III), Sm(III), and Nd(III) complexes were recorded over the scanning angle of 2θ= 10º–90º range. The complex of Pr(III) exhibited a diffractogram with sharp peaks designating the crystalline nature of the complex **(Fig. 6)**. All the other complexes, viz., La(III), Ce(III), Sm(III), and Nd(III) complexes, produced diffractograms having no well-defined crystalline peaks indicating that all these complexes are amorphous in nature. Attempts to prepare the single crystals of the complexes were unsuccessful and hence the exact crystal structure could not be determined. The information in the powder XRD pattern of $Pr(N_2H_5)(tdp)_2 \cdot H_2O$ was also not sufficient to get the crystal structure of the complex and more detailed investigation is needed to get the crystal structure of the complexes.

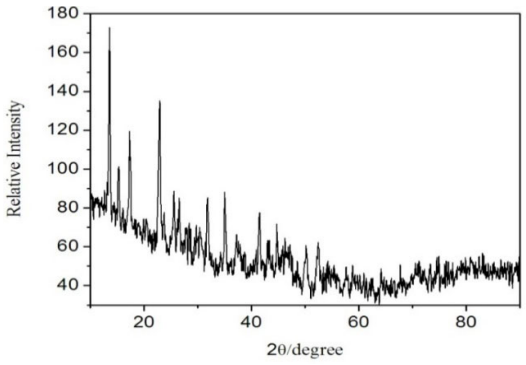

Fig. 6. XRD pattern of $Pr(N_2H_5)(tdp)_2 \cdot H_2O$ complex.

Based on all the above results, the molecular structures given in **Fig. 7** are proposed for the synthesized complexes.

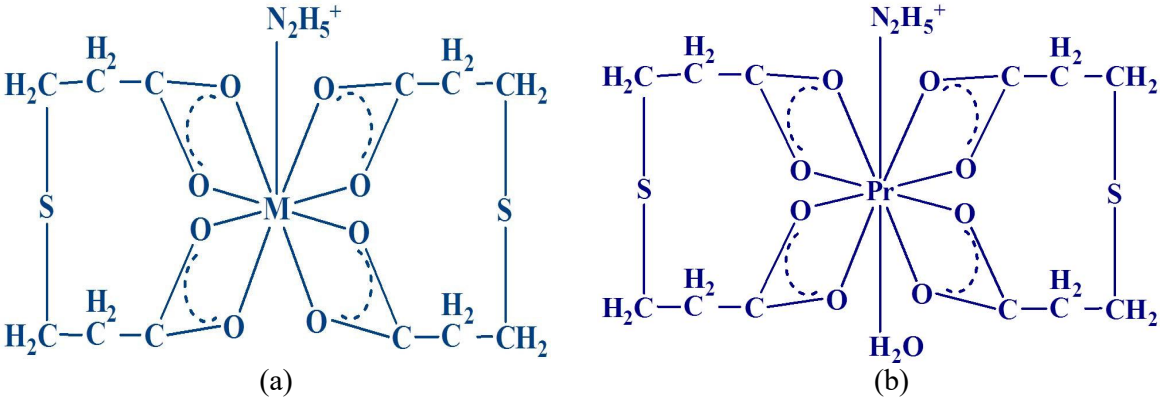

Fig. 7. Proposed structure of (a) $M(III)(N_2H_5)(tdp)_2$ where M = La, Ce, Sm and Nd; (b) $Pr(III)(N_2H_5)(tdp)_2 \cdot H_2O$.

2.6. SEM analysis

The surface morphological structures (particle size and shape) of the powder complexes were studied by SEM (Scanning Electron Microscopy) analysis and the recorded images are given in **Fig. 8**. The instrumental parameters, magnification, working distance, and accelerating voltage are designated in the SEM image. It is clear from **Fig. 8** that the particles are not highly crystalline, and they have smooth glassy surfaces which confirms the XRD results that these complexes possess crystalline–amorphous composite nature.

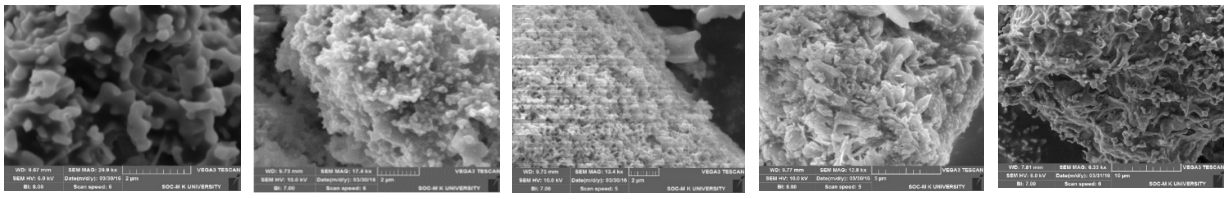

Fig. 8. SEM photographs of (a) La(III), (b) Ce(III), (c) Sm(III), (d) Pr(III) and (e) Nd(III) complexes.

SEM studies were also carried out for the metal oxides obtained from the complexes after decomposition at 1300 °C for 1 h in a muffle furnace. The SEM image of the oxide residue obtained from $Pr(N_2H_5)(tdp)_2 \cdot H_2O$ is shown in **Fig. 9**. This led us to the inference that the residue is a submicron-sized metal oxide with a sponge structure and the complexes may be used as a precursor for nanometal oxides preparation.[48]

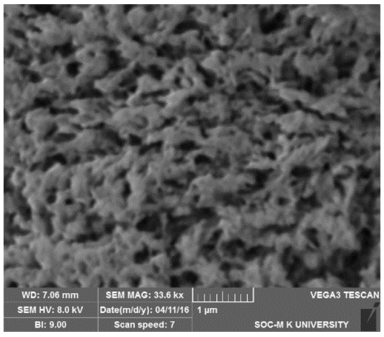

Fig. 9. SEM image of Pr_2O_3 obtained using $Pr(N_2H_5)(tdp)_2 \cdot H_2O$.

2.7. Antimicrobial Activities

2.7.1. Antibacterial activity

Antibacterial activity of the 3,3'-thiodipropanoic acid (H_2tdp) and its lanthanide (La(III), Ce(III), Sm(III), Pr(III), and Nd(III)) metal complexes were screened by the disc diffusion method, against the selected human pathogenic bacterial strains, viz., *Bacillus cereus, Staphylococcus aureus, Proteus vulgaris, Pseudomonas aeruginosa, Escherichia coli,* and *Serratia species*. The antibacterial study results are in **Table S5**, **Fig. S4,** and **Fig. 10**. The observation of the higher antibacterial activity of the lanthanide metal complexes when compared with free ligands might originate from the structural changes upon coordination and chelating to make metal complexes. Hence, it is reflected in the form of more dominant and prevailing bacteriostatic activity consequently inhibiting the growth of the bacteria.[49, 50] This increase in the activity of the complexes is in line with the basis of the chelation theory.[51] The entire complexes used in this investigation showed very good bactericidal activities with a zone of inhibition of 16–22 mm against *B. cereus* than the other microorganisms. Further, all the complexes showed moderate antibacterial activity against *P. aeruginosa* (13–19 mm), *S. aureus* (12–17 mm), and *P. vulgaris* (9–13 mm). Further, all complexes with the exception of Pr(III) complex displayed no activity against *E. coli* and *S. species* microorganisms.

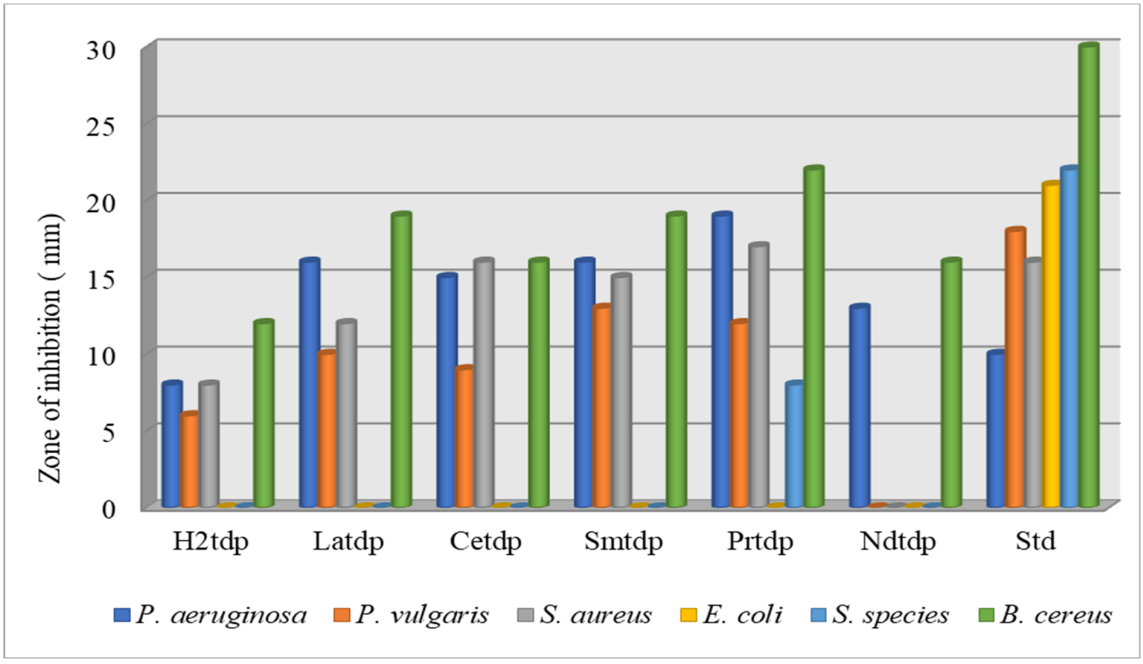

Fig. 10. Antibacterial activity of the ligand and the complexes.

The *in vitro* minimum inhibitory concentration (MIC) of ligand and the synthesized compounds against *P. vulgaris, P. aeruginosa, B. cereus,* and *S. aureus* bacterial strains were assessed, and the results are given in **Table 2**. All the compounds were used at a concentration ranging from 0.003 to 0.5 mg/mL against the bacterial strains tested. The MIC values revealed that all the complexes possess very good activity compared to the ligand against mentioned microbes, and this activity was found to be enriched due to coordination with the metal ions. For instance, the Pr(III) complex showed much better activity with a MIC value of 0.031 mg/mL against *B. cereus.* The Sm(III) and Nd(III) complexes showed moderate activity with a MIC value of 0.062 mg/mL against *B. cereus*.

Table 2. Minimum inhibitory concentration assay of the complexes and standard antibiotic against bacterial strains

Compound	**Minimum inhibitory concentration(mg/mL)**			
	Gram-negative		Gram-positive	
	P. vulgaris	*P. aeruginosa*	*B. cereus*	*S. aureus*
H_2tdp	0.5	0.5	0.5	0.5
La(N_2H_5)(tdp)$_2$	0.5	0.125	0.25	0.5
Ce(N_2H_5)(tdp)$_2$	0.5	0.25	0.25	0.25
Sm(N_2H_5)(tdp)$_2$	0.5	0.5	0.062	0.125
Pr(N_2H_5)(tdp)$_2$·H_2O	0.5	0.125	0.031	0.25
Nd(N_2H_5)(tdp)$_2$	ND	0.5	0.062	ND
Streptomycin (Std)	0.003	0.003	0.0025	0.001

ND = Not done for MIC test. (No activity in disc diffusion assay)

2.7.2. In vitro antifungal activity

In vitro, antifungal activities of 3,3'-thiodipropanoic acid (H_2tdp) and its metal complexes were studied against four fungi, namely, *Candida albicans, Aspergillus niger*, *Aspergillus fumigatus* and *Penicilium variance* and were compared with the activity of a standard antifungal drug Ketoconazole at the same concentration and the obtained results are given in **Table S6**, **Fig. S5** and **Fig. 11**. The *in vitro* antifungal activity data indicates that some metal complexes are more active when compared with the free ligand. All the hydrazine metal complexes displayed remarkable antifungal activity against *C. albicans*, *A. fumigatus,* and *P. variance* which is comparable to the activity of the standard drug Ketoconazole. The complex of Nd(N_2H_5)(tdp)$_2$ has displayed very good antifungal activity (18 mm) against *P. variance* microorganism. Among all the prepared complexes, the complex La(N_2H_5)(tdp)$_2$ has shown higher antifungal activity (23 mm) than the standard drug Ketoconazole against *A. fumigatus* fungi. The effective antifungal activity of synthesized complexes compared to the corresponding ligand can be described based on chelation theory. The polarity of the metal ion will be reduced to a greater extent upon chelation due to the overlap of the ligand orbital and partial sharing of the charge of the metal ion with donor groups. It increases the delocalization of π-electrons over the whole chelating ring and enhances the penetration of the complexes into lipid membranes and blocks the metal binding sites in the enzymes of microorganisms. Thus, these complexes disturb the respiration process of the cell and block the synthesis of proteins, which restricts further growth of microorganism.[52]

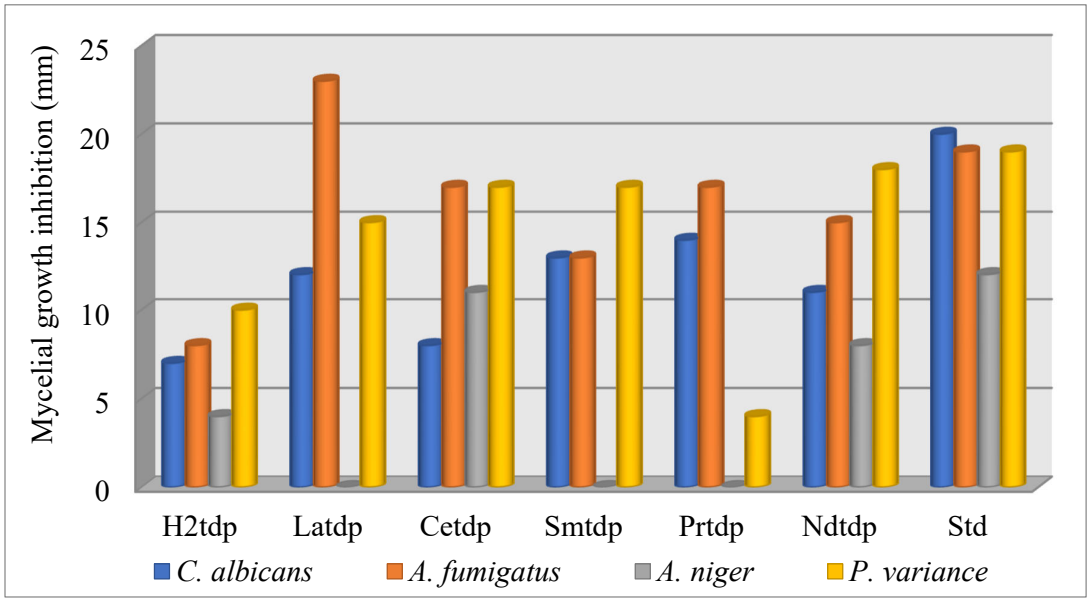

Fig. 11. Antifungal activity of the ligand and the complexes.

3. Conclusions

The reaction between the solutions of rare earth metal nitrates and the mixture of hydrazine and 3,3'-thiodipropanoic acid yielded complexes of the formulae, $M(N_2H_5)(tdp)_2$ where M = La, Ce, Sm, and Nd and $Pr(N_2H_5)(tdp)_2{\cdot}H_2O$. The analytical and mass, electronic, FTIR and Raman spectroscopic data support the formulated molecular formulae of the complexes. The IR spectroscopic data of the complexes indicate the bidental coordination of both the carboxylate groups of 3,3'-thiodipropanoic acid with metals and the monodentate coordination of hydrazine. All the complexes undergo thermal decomposition in three steps. Hydrazine decomposes in the initial step followed by the decomposition of organic moiety in the second step to give the respective metal oxalates, which on further decomposition give the metal carbonates. Pr(III) complex alone contains coordinated water molecules. Results obtained from powder XRD suggested that the complexes were amorphous in nature which is further supported by SEM results. Since the complexes were insoluble in any solvent due to their polymeric nature, single crystals could not be prepared. Based on the analytical, spectral, and thermal studies, nine coordination around Ln^{3+} ions (La^{3+}, Ce^{3+}, Sm^{3+}, and Nd^{3+}) was assigned with an exception for the praseodymium complex which holds ten-coordination around the metal ion. The newly prepared hydrazine rare earth metal (La^{3+}, Ce^{3+}, Sm^{3+}, Pr^{3+}, and Nd^{3+}) complexes exhibit very good antibacterial and antifungal activity against the tested microbes. The complex $[Pr(N_2H_5)(tdp)_2{\cdot}H_2O]$ showed the best antibacterial activity with a MIC value of 0.031 mg/mL against *B. cereus* bacteria and $[La(N_2H_5)(tdp)_2]$ complex exhibited the maximum antifungal activity (23 mm) against *A. fumigatus* fungus.

Acknowledgments

The author K. K is thankful to the University Grants Commission, New Delhi, India, for the award of the BSR Jounior Research Fellowship. The authors thank UGC, New Delhi for providing a Micro-Raman facility through the UPE programme. DST, Gov't of India, New Delhi is gratefully acknowledged for the instrumental facilities provided through DST-FIST and DST-PURSE programmes.

4. Experimental

4.1. Materials

Analytical grade chemicals of 3,3'-Thiodipropionic acid (Alfa Aesar, 98%), Lanthanum(III) nitrate hexahydrate (Merck, 99.99%), Cerium(III) nitrate hexahydrate (Alfa Aesar, 99.5%), Praseodymium(III) nitrate hexahydrate (Alfa Aesar, 99.99%), Samarium(III) nitrate hexahydrate (Sigma Aldrich, 99.9%,), Neodymium(III) nitrate hexahydrate (Sigma Aldrich, 99.99%) were used as received and the solvents were freshly distilled before use. Hydrazine hydrate of 99–100% purity, received from Merck, was used in all the chemical reactions.

4.2. Characterization techniques

The hydrazine content in the newly synthesized complexes was determined volumetrically by titrating with 0.025 M potassium iodate solution using Andrew's conditions.[53] The amount of metal present in the complexes was determined by ICP-OES and AAS techniques using Perkin Elmer optima 5300 DV ICP-OES spectrometer and HP 3510 atomic absorption spectrometer, respectively. Elemental analysis was performed on a Perkin Elmer-240 B CHN analyzer. ESI–mass spectral analysis was performed on a liquid chromatography-ion trap mass spectrometer (LCQ Fleet, Thermo Fisher Instruments Limited, US) in both positive and negative ion mode. The solid-state UV-vis absorption spectra of the metal complexes were recorded on a UV-visible spectrophotometer (Shimadzu, model 2450) equipped with a diffuse relectance accessory. FT-IR spectra were recorded on a JASCO 460 plus FT-IR spectrometer using the KBr pellet method in the range of 4000–400 cm^{-1}. Raman spectra were acquired by exciting the sample with a 633 nm He–Ne laser and measuring in 180° backscattering geometry using a spectrometer (LabRamHR800) equipped with a CCD detector device. The simultaneous TGA–DTA was performed on a Perkin Elmer STA 6000 thermal analyzer using platinum cups as sample holders with 8–9 mg of the sample at a heating rate of 10 °C/min in a nitrogen atmosphere. The powder XRD patterns of the complexes were recorded with a JEOL JDX 8030 X-ray diffractometer using CuKa radiation along nickel filter. The SEM with energy dispersive X-ray analysis was carried out on a TESCAN VEGA3 scanning electron microscope.

4.3. Synthesis of $M(N_2H_5)(tdp)_2$, where M = La, Ce, Sm and Nd, and $Pr(N_2H_5)(tdp)_2{\cdot}H_2O$

3,3'-thiodipropanoic acid (0.356 g, 0.002 mol) and hydrazine hydrate (0.100 mL, 0.002 mol) were added to a beaker containing 50 mL of double distilled water. This solution was vigorously stirred and heated over a water bath (30 minutes) at 90 °C to get a clear solution with pH 8. Then, it was added gently to an aqueous solution containing 0.002 mol of the corresponding metal nitrate hexahydrate (e.g. 0.866 g of $(La(NO_3)_3{\cdot}6H_2O)$, 0.002 mol) with continuous stirring. This final solution was concentrated over a water bath at 80–90 °C to reduce the volume of the solution to about 10 mL and then permitted to stand for one day at room temperature condition. The formed polycrystalline solids were filtered using G4

sintered crucible and washed with double distilled water, methanol followed by ether, and finally dried at 40 °C in a vacuum oven.

4.4. Antibacterial activity

3,3'-thiodipropanoic acid (H_2tdp) and its synthesized La^{3+}, Ce^{3+}, Pr^{3+}, Nd^{3+}, and Sm^{3+} complexes were subjected to their *in vitro* antibacterial activity, using the disc diffusion method.[54] All these complexes were tested against two gram-positive bacterial strains *Bacillus cereus* (Strain No. ATCC14579) and *Staphylococcus aureus* (MTCC1144), and four gram-negative bacterial strains, namely, *Proteus vulgaris* (ATCC13315), *Escherichia coli* (ATCC25922), *Serratia species* (ATCC39006), *Pseudomonas aeruginosa* (ATCC15442). Bacterial strains were cultured on nutrient broth for 24 hours, at 37 °C. 40 µL of (1 ppm solution) aseptically synthesized complexes (filter sterilized with 0.45µ) were impregnated on a sterile filter paper disc (6 mm) and placed on Muller Hinton broth plates seeded with 0.1 mL of 10^6 colony forming units per mL (CFU/mL) bacterial cultures. All the prepared plates were incubated at 37 °C for 24 hours. Methanol with acetylacetone and Streptomycin (10 µg) was used as a solvent control and standard antibiotic, respectively. After incubation for 24 hours, the zone of inhibition was measured in millimeters (mm).

The lowest concentration where no visible bacterial turbidity is observed in the test tubes is known as Minimum Inhibitory Concentration (MIC).[55] MIC of all the compounds was determined by micro dilution method agreeing to the National Committee for Clinical Laboratory Standards.[56] Standardized suspension of test bacteria (10^6 CFU/mL) and 3,3'-thiodipropanoic acid and its La(III), Ce(III), Sm(III), Pr(III), and Nd(III) complexes were prepared using methanol and acetyl acetone solvent system. The Minimum Inhibitory Concentration was determined in a 96 well test plate filled with Muller-Hinton broth medium and various concentrations (0.5, 0.25, 0.125, 0.062, 0.031, 0.015, and 0.007 mg/mL) of reference drug (or) the ligand (or) the prepared complexes. The solvent was used as a negative control. 100 µL of new bacterial broth suspension (10^6 CFU/mL) was added to each of the wells without changing the dilution factor. The complete assay was arranged in triplicate in 96 well MIC plates and incubated at 37 °C for 24 h. Using 96 well plate readers (ELISA Plate reader), the bacterial growth was measured by optical density (OD) at 600 nm and by the visual appearance of turbidity.

4.5. In vitro antifungal activity

The anti-fungal activity of the ligand and synthesized metal complexes were tested against four different fungi, namely, *Candida albicans* (Strain No. ATCC10231), *Aspergillus niger* (ATCC16404), *Aspergillus fumigatus* (ATCC MYA-3626) and *Penicilium variance* (KU305735), using the agar well diffusion method.[57] The fungal strains were grown on potato dextrose agar (PDA) at 25 °C for 7 days. One week old fungal culture was used as inoculum for studying the anti-fungal activity of the test compounds. Ketoconazole and methanol–acetylacetone solvent systems were used as a reference antifungal drug and negative control, respectively. Solutions of the test compounds and the standard drug were prepared in methanol/acetyl acetone at a concentration of 1 mg mL^{-1}. Sterilized potato dextrose agar was poured onto petri plates. In each plate, different test fungal cultures were swabbed over the agar surface using the sterile cotton swab. Wells were prepared on the agar surface using the sterile gel puncture and about 120 µL of the test samples were loaded onto the wells. All the inoculated plates were incubated for 3 days at room temperature and the *in vitro* antifungal result of the test solutions was observed in the form of circular zones of inhibition.

References

1. Younis S. A., Bhardwaj N., Bhardwaj S. K., Kim K. H., and Deep A. (**2021**) Rare earth metal–organic frameworks (RE-MOFs): Synthesis, properties, and biomedical applications. *Coord. Chem. Rev.*, 29, 213620. (DOI: https://doi.org/10.1016/j.ccr.2020.213620).
2. Chundawat N. S., Jadoun S., Zarrintaj P., and Chauhan N. P. S. (**2021**) Lanthanide complexes as anticancer agents. *Polyhedron*, 207, 115387. (DOI: https://doi.org/10.1016/j.poly.2021.115387).
3. Kaczmarek M. T., Zabiszak M., Nowak M., and Jastrzab R. (**2018**) Lanthanides: Schiff base complexes, applications in cancer diagnosis, therapy, and antibacterial activity. *Coord. Chem. Rev.*, 370, 42-54. (DOI: https://doi.org/10.1016/j.ccr.2018.05.012).
4. Gaoa S., Huanga M., Suna Z., Li D., Xiea C., Fenga L., Liua S., Zhenga K., and Pang Q. (**2021**) A new mixed-ligand lanthanum(III) complex with salicylic acid and 1,10-phenanthroline: Synthesis, characterization, antibacterial activity, and underlying mechanism. *J. Mol. Struct.,* 1225, 129096. (DOI: https://doi.org/10.1016/j.molstruc.2020.129096).
5. Taha Z. A., Ababneh T. S., Hijazi A. K., AL-Aqtash S. M., Al-Momani W. M., and Mhaidat I. (**2022**) Synthesis, spectral characterization, thermal, computational and antibacterial studies of lanthanide complexes with 2-fluorobenzoic acid-(5-R-2-hydroxy-benzylidene) hydrazide {R = chloro or bromo). *J. Saudi Chem. Soc.,* 26, 101400. (DOI: https://doi.org/10.1016/j.jscs.2021.101400).
6. Aime S., and Baranyai Z. (**2022**) How the catalysis of the prototropic exchange affects the properties of lanthanide(III) complexes in their applications as MRI contrast agents. *Inorg. Chim. Acta*, 532, 120730. (DOI: https://doi.org/10.1016/j.ica.2021.120730).
7. Franklin S. J. (**2001**) Lanthanide-mediated DNA hydrolysis. *Curr. Opin. Chem. Biol.,* 5, 201–208. (DOI: https://doi.org/10.1016/S1367-5931(00)00191-5).

8. Geng S., Ren N., He S. M., and Zhang J. J. (**2022**) Synthesis and structural characterization of lanthanide metal complexes by 2-fluorobenzoic acid with 2,2′:6′,2″-terpyridine, and their fluorescence properties. *J. Mol. Struct.,* 1252, 132165. (DOI: https://doi.org/10.1016/j.molstruc.2021.132165).
9. Belousov Y. A., Drozdov A. A., Taydakov I. V., Marchetti F., Pettinari R., and Pettinari C. **(2021)** Lanthanide azolecarboxylate compounds: Structure, luminescent properties and applications. *Coord. Chem. Rev.,* 445, 214084. (DOI: https://doi.org/10.1016/j.ccr.2021.214084).
10. Navarro A. C., Romero D. H., Parra A. F., Rivera J. M., Blum S. E. C., and Peralta R. C. **(2021)** Structural diversity and luminescent properties of coordination complexes obtained from trivalent lanthanide ions with the ligands: *tris*((1*H*-benzo[*d*]imidazol-2-yl)methyl)amine and 2,6-*bis*(1*H*-benzo[*d*]imidazol-2-yl)pyridine. *Coord. Chem. Rev.,* 427, 213587. (DOI: https://doi.org/10.1016/j.ccr.2020.213587).
11. Barkanov A., Zakharova A., Vlasova T., Barkanova E., Khomyakov A., Avetissov I., Taydakov I., Datskevich N., Goncharenko V., and Avetisov R. (**2022**) NIR-OLED structures based on lanthanide coordination compounds: synthesis and luminescent properties. *J. Mater. Sci.,* 57, 8393–8405. (DOI: https://doi.org/10.1007/s10853-021-06721-4).
12. Guerra R. B., Galico D. A., Silva T. F. C. F., Aguiar J., Venturini J., and Bannach G. (**2021**) Rare-earth complexes with anti-inflammatory drug sulindac: Synthesis, characterization, spectroscopic and in vitro biological studies*, Inorg. Chim. Acta,* 526, 120516. (DOI: https://doi.org/10.1016/j.ica.2021.120516).
13. Yamin A. A. A., Abduh M. S., Saghir S. A. M., and gabri N. A. (**2022**) Synthesis, Characterization and Biological Activities of New Schiff Base Compound and Its Lanthanide Complexes. *Pharmaceuticals,* 15(4), 454. (DOI: https://doi.org/10.3390/ph15040454).
14. Kapoor P., Fahmi N., and Singh R. V. **(2011**) Microwave assisted synthesis, spectroscopic, electrochemical and DNA cleavage studies of lanthanide(III) complexes with coumarin based imines. *Spectrochim. Acta A,* 83, 74–81. (DOI: https://doi.org/10.1016/j.saa.2011.07.054).
15. Zong G. C., Huo J. X., Ren N., Zhang J. J., Qi X. X., Gao J., Geng L. N., Wang S. P., and Shi S. K. (**2015**) Preparation, characterization and properties of four new trivalent lanthanide complexes constructed using 2-bromine-5-methoxybenzoic acid and 1,10-phenanthroline. *Dalton Trans*., 44, 14877–14886. (DOI: https://doi.org/10.1039/C5DT01969A).
16. Tiwary S. K., Prakash R., and Rathore D. P. S. (**1978**) Metal complexes of thiopolycarboxylic acid Co(II), Ni(II), Cu(II) and Cr(III) complexes with 3,3-thiodipropionic acid. *J. Indian Chem. Soc.,* 55, 537–538.
17. Cheng H. J., Shen Y. L., Zhang S. Y., Ji H. W., Yin W. Y., Li . K., and Yuan R. X. (**2015**) Three Coordination Polymers Constructed with Zinc(II), 3,3′-Thiodipropionic Acid, and Bipyridyl Ligands: Syntheses, Crystal Structures and Luminescent Properties. *Z. Anorg. Allg. Chem.,* 641, 1575–1580. (DOI: https://doi.org/10.1002/zaac.201500167).
18. Chandra S., and Sharma A. K. (**2009**) Synthesis, Thermal Behaviour, XRD, and Luminescent Properties of Lighter Lanthanidethiodipropionate Hydrates Containing Aminogunidine as Neutral Ligand. *Res. Lett. Inorg. Chem.*, *Article* ID: 945670. (DOI: https://doi.org/10.1155/2009/945670 .
19. Packiaraj S., and Govindarajan S. (**2014**) Synthesis, Thermal Behaviour, XRD, and Luminescent Properties of Lighter Lanthanidethiodipropionate Hydrates Containing Aminogunidine as Neutral Ligand*. Open J. Inorg. Chem.,* 4, 41–49. (DOI: https://doi.org/10.4236/ojic.2014.43006).
20. Chlebda D. K., Jedrzejczyk R.J., Jodlowski P. J., and Lojewska J. (**2017**) Surface structure of cobalt, palladium, and mixed oxide-based catalysts and their activity in methane combustion studied by means of micro-Raman spectroscopy. *J. Raman Spectrosc*., 1-10. (DOI: https://doi.org/10.1002/jrs.5261).
21. Jodlowski P. J., Chlebda D., Piwowarczyk E., Chrzan M., Jedrzejczyk R. J., Sitarz M., Wegrzynowicz A., Kolodziej A., and Lojewska J. (**2016**) In situ and operando spectroscopic studies of sonically aided catalysts for biogas exhaust abatement, *J. Mol. Struct*., 1126, 132-140. (DOI: https://doi.org/10.1016/j.molstruc.2016.02.039).
22. Lojewskaa J., Knapika A., Jodlowski P., Lojewski T., and Kolodziej A. (**2013**) Topography and morphology of multicomponent catalytic materials based on Co, Ce and Pd oxides deposited on metallic structured carriers studied by AFM/Raman interlaced microscopes. *Catal. Today*, 216, 11-17. (DOI: https://doi.org/10.1016/j.cattod.2013.05.008).
23. Chlebda D. K., Stachurska P., Jedrzejczyk R. J., Kuterasinski L., Dziedzicka A., Sylwia G., Chmielarz L., Lojewska J., Sitarz M., and Jodowski P. J. (**2018**) DeNO$_x$ Abatement over Sonically Prepared Iron-Substituted Y, USY and MFI Zeolite Catalysts in Lean Exhaust Gas Conditions. *Nanomaterials*, 8(1), 21. (DOI: https://doi.org/10.3390/nano8010021).
24. Jodlowski P.J., Chlebda D. K., Jedrzejczyk R. J., Dziedzicka A., Kuterasinski L., and Sitarz M. (**2017**) Characterisation of well-adhered ZrO_2 layers produced on structured reactors using the sonochemical sol-gel method. *Appl. Surf. Sci*., 427, 563-574. (DOI: https://doi.org/10.1016/j.apsusc.2017.08.057).
25. Heaton B. T., Jacob C., and Page P. (**1996**) Transition metal complexes containing hydrazine and substituted hydrazines. *Coord. Chem. Rev.,* 154, 193–229. (DOI: https://doi.org/10.1016/0010-8545(96)01285-4).
26. Premkumar T., and Govindarajan S. (**2010**) Thermoanalytical and spectroscopic studies on hydrazinium lighter lanthanide complexes of 2-pyrazinecarboxylic acid. *J. Therm. Anal. Calorim.,* 100, 725–732. (DOI: https://doi.org/10.1007/s10973-009-0117-1).
27. Vikram L., and Sivasankar B. N. (**2008**) Hydrazinium metal(II) and metal(III) ethylenediamine tetraacetate hydrates. *J. Therm. Anal. Calorim.,* 91, 963–970. (DOI: https://doi.org/10.1007/s10973-007-8612-8).
28. Gonsalves L. R., Verenkar V. M. S., and Mojumdar S. C. (**2009**) Preparation and characterization of $Co_{0.5}Zn_{0.5}Fe_2(C_4H_2O_4)_3 \cdot 6N_2H_4$. *J. Therm. Anal. Calorim.,* 96, 53–57. (DOI: https://doi.org/10.1007/s10973-008-9837-x).
29. Raju B., and Sivasankar B. N. (**2008**) Spectral, thermal and X-ray studies on some new *Bis*-hydrazine lanthanide(III) glyoxylates. *J. Therm. Anal. Calorim.,* 94, 289–296. (DOI: https://doi.org/10.1007/s10973-007-8953-3).
30. Ravindranathan P., and Patil K. C. (**1983**) Thermal reactivity of metal formate hydrazinates. *Thermochim. Acta,* 71, 53–57. (DOI: https://doi.org/10.1016/0040-6031(83)80354-2).
31. Mahesh G. V., and Patil K. C. (**1983**) Thermal reactivity of metal acetate hydrazinates. *Thermochim. Acta,* 99, 153–158. (DOI: https://doi.org/10.1016/0040-6031(86)85277-7).

32. Sivasankar B. N., and Govindarajan S. (**1994**) *Z. Naturforsch.,* 49b, 950–954. (DOI: https://doi.org/10.1515/znb-1994-0716).
33. Sivasankar B. N., and Govindarajan S. (**1994**) Tris-hydrazine metal glycinates and glycolates: Preparation, spectral and thermal studies. *Thermochim. Acta,* 244, 235–242. (DOI: https://doi.org/10.1016/0040-6031(94)80222-X).
34. Kuppusamy K., and Govindarajan S. (**1996**) Synthesis, spectral and thermal studies of some 3d-metal hydroxybenzoate hydrazinate complexes. *Thermochim. Acta,* 274, 125–138. (DOI: https://doi.org/10.1016/0040-6031(95)02700-9).
35. Vairam S., Premkumar T., and Govindarajan S. (**2010**) Trimellitate complexes of divalent transition metals with hydrazinium cation. *J. Therm. Anal. Calorim.,* 100, 955–960. (DOI: https://doi.org/10.1007/s10973-009-0459-8).
36. Vairam S., Premkumar T., and Govindarajan S. (**2010**) Preparation and thermal behaviour of divalent transition metal complexes of pyromellitic acid with hydrazine. *J. Therm. Anal. Calorim.,* 101, 979–985. (DOI: https://doi.org/10.1007/s10973-009-0433-5).
37. Arunadevi N. (**2009**) [Ph.D thesis], Anna university, Chennai, India.
38. Arunadevi N., Devipriya S., and Vairam S. (**2009**) Hydrazinium metal 1-hydroxy-2-naphthoates—new precursors for metal oxides. *Inter. J. Engg. Sci. Tech.,* 3, 1–8.
39. Grirrane A., Alvarez E., Pastor A., and Galindo A. (**2010**) Thiodipropionate Zn^{II} Complexes: Synthesis, DFT Studies, and X-ray Structure of $[\{Zn(phen)(H_2O)\}_2(\mu\text{-tdp})_2]\cdot 3H_2O$. *Z. Anorg. Allg. Chem.,* 636, 2409–2412. (DOI: https://doi.org/10.1002/zaac.201000145).
40. Yang P. P., Li. B., Wang Y. H., Gu W., and Liu X. (**2008**) Synthesis, Structure, and Luminescence Properties of Zinc(II) and Cadmium(II) Complexes containing the Flexible Ligand of 3,3′-Thiodipropionic Acid. *Z. Anorg. Allg. Chem.,* 634, 1221–1224. (DOI: https://doi.org/10.1002/zaac.200700597).
41. Arici M., Yesilel O. Z., Keskin S., and Tas M. (**2012**) A three-dimensional silver(I) framework assembled from 3,3′-thiodipropionate: Synthesis, structure and molecular simulations for hydrogen gas adsorption. *Polyhedron,* 45, 103–106. (DOI: https://doi.org/10.1016/j.poly.2012.07.060).
42. Arici M., Yesilel O. Z., Sahin O., and Buyukgungor O. (**2014**) Two dimensional coordination polymers with 3,3′-thiodipropionate: An unprecedented coordination mode and strong hydrogen-bond network. *Polyhedron,* 67, 456–463. (DOI: https://doi.org/10.1016/j.poly.2013.09.040).
43. Brzyska W., and Ozga W. (**1996**) Preparation and properties of Y(III) and lanthanide(III) complexes with pyridine-2,4-dicarboxylic acid. *Thermochim. Acta,* 273, 205–216. (DOI: https://doi.org/10.1016/0040-6031(95)02393-3).
44. Braibanti A., Dallavalle F., Pellingheli M. A., and Laporati E. (**1968**) The nitrogen-nitrogen stretching band in hydrazine derivatives and complexes. *Inorg. Chem.* 7, 1430–1433 (DOI: https://doi.org/10.1021/ic50065a034).
45. Tiwari S. K., and Rathore D. P. S. (**1979**) Metal-complexes of thiopolycarboxylic acid - magnetic and spectral studies of zinc(II), cadmium(II), mercury(II), manganese(II) and iron(III) complexes with thiodisuccinic acid. *Natl. Acad. Sci. Lett.,* 8, 293–296.
46. Reisfeld R., and Jorgensen C. K. (**1977**) Lasers and Excited States of Rare Earths. *Springer-Verlag,* Berlin, pp 64–122. (DOI: https://doi.org/10.1007/978-3-642-66696-4-2).
47. Carnall W. T., Fields P. R., and Rajnak K. (**1968**) Spectral Intensities of the Trivalent Lanthanides and Actinides in Solution. II. Pm^{3+}, Sm^{3+}, Eu^{3+}, Gd^{3+}, Tb^{3+}, Dy^{3+}, and Ho^{3+}. *J. Chem. Phys.,* 49, 4412–4423. (DOI: https://doi.org/10.1063/1.1669892).
48. Patil K. C. (**1986**) Metal-hydrazine complexes as precursors to oxide materials. *J. Chem. Sci.,* 96, 459–464. (DOI: https://doi.org/10.1007/BF02936298).
49. Shanker K., Rohini R., Ravinder V., and Reddy P. M. (**2009**) Ru(II) complexes of N_4 and N_2O_2 macrocyclic Schiff base ligands: Their antibacterial and antifungal studies. *Spectrochim. Acta A,* 73, 205–211. (DOI: https://doi.org/10.1016/j.saa.2009.01.021).
50. Atabay N. M. A., Dulger B., and Gucin F. (**2005**) Structural characterization and antimicrobial activity of 1,3-bis(2-benzimidazyl)-2-thiapropane ligand and its Pd(II) and Zn(II) halide complexes. *Eur. J. Med. Chem.,* 40, 1096–1102. (DOI: https://doi.org/10.1016/j.ejmech.2005.05.006).
51. Tweedy B. G. (**1964**) Plant Extracts with Metal Ions as Potential Antimicrobial Agents. *Phytopathology,* 55, 910–914.
52. Dharmaraj N., Viswanathamurthi P., and Natarajan K. (**2002**) Ruthenium(II) complexes containing bidentate Schiff bases and their antifungal activity. *Trans. Met. Chem.,* 26, 105–109. (DOI: https://doi.org/10.1023/A:1007132408648).
53. Vogel A. I. (**1975**) Volumetric (titrimetric) analysis. In A Text Book of Quantitative Inorganic Analysis, 3rd edn. Longman, London, p 380.
54. Murray P. R., Baron E. J., Pfaller M. A., Tenover F. C., and Yolke R. H. (**1995**) Manual of Clinical Microbiology, ASM, Washington, DC, p 6.
55. Londonkar R. L., Kattegouga U. M., Shivsharanappa K., and Hanchinalmath J. V. (**2013**) Phytochemical screening and in vitro antimicrobial activity of *Typha angustifolia* Linn leaves extract against pathogenic gram-negative microorganisms. *J. Pharm. Res.,* 6, 280–283. (DOI: https://doi.org/10.1016/j.jopr.2013.02.010).
56. NCCLS (National Committee for Clinical Laboratory Standards) (**1997**) Performance Standards for Antimicrobial Disc Susceptibility Test, Approved Standard M2-A6, NCCLS, 6th edn, Wayne, Pa, USA.
57. Perez C., Paul M., and Bezique P. (**1990**) An Antibiotic assay by the agar well diffusion method. *Alta. Biomed. Group Experiences,* 15, 113.